ESTIMATION OF STRETCH REFLEX CONTRIBUTIONS OF WRIST USING SYSTEM IDENTIFICATION AND QUANTIFICATION OF TREMOR IN PARKINSON'S DISEASE PATIENTS

by

Sushant Tare

B.E. in Instrumentation engineering, University of Mumbai, 2005

Submitted to the Graduate Faculty of

The Swanson School of Engineering in partial fulfillment

of the requirements for the degree of

M.S. in Electrical Engineering

University of Pittsburgh

2009

UNIVERSITY OF PITTSBURGH

SWANSON SCHOOL OF ENGINEERING

This thesis was presented

by

Sushant Tare

It was defended on

March 20, 2009

and approved by

Zhi-Hong Mao, PhD, Assistant Professor, Department of Electrical and Computer Engineering

Ching-Chung Li, PhD, Professor, Department of Electrical and Computer Engineering

Luis F. Chaparro, PhD, Associate Professor, Department of Electrical and Computer Engineering

Thesis Advisor: Zhi-Hong Mao, PhD, Assistant Professor, Department of Electrical and Computer Engineering

ESTIMATION OF STRETCH REFLEX CONTRIBUTIONS OF WRIST USING SYSTEM IDENTIFICATION AND QUANTIFICATION OF TREMOR IN PARKINSON'S DISEASE PATIENTS

Sushant Tare, M.S.

University of Pittsburgh, 2009

"The brain's motor control can be studied by characterizing the activity of spinal motor nuclei to brain control, expressed as motor unit activity recordable by surface electrodes" [1]. When a specific area is under consideration, the first step in investigation of the motor control system pertinent to it is the system identification of that specific body part or area. The aim of this research is to characterize the working of the brain's motor control system by carrying out system identification of the wrist joint area and quantifying tremor observed in Parkinson's disease patients. We employ the ARMAX system identification technique to gauge the intrinsic and reflexive components of wrist stiffness, in order to facilitate analysis of problems associated with Parkinson's disease. The intrinsic stiffness dynamics comprise majority of the total stiffness in the wrist joint and the reflexive stiffness dynamics contribute to the tremor characteristic commonly found in Parkinson's disease patients. The quantification of PD tremor entails using blind source separation of convolutive mixtures to obtain sources of tremor in patients suffering from movement disorders. The experimental data when treated with blind source separation reveals sources exhibiting the tremor frequency components of 3-8 Hz. System identification of stiffness dynamics and assessment of tremor can reveal the presence of additional abnormal neurological signs and early identification or diagnosis of these symptoms would be very advantageous for clinicians and will be instrumental to pave the way for better treatment of the disease.

TABLE OF CONTENTS

ACKNOWLEDGEMENTS ..... **IX**

1.0 INTRODUCTION **1**

2.0 ANALYSIS METHODS **4**

2.1 TEST DESCRIPTION **4**

2.1.1 Instrumentation **4**

2.1.2 Perturbation Signal Design **5**

2.1.3 Test Subjects **6**

2.1.4 Testing Protocol **7**

2.2 PARALLEL WRIST STIFFNESS DYNAMICS **7**

2.2.1 Intrinsic Stiffness **8**

2.2.2 Reflexive Stiffness **9**

2.2.3 Reflexive Component Delay **10**

2.3 PARAMETRIC ESTIMATION **10**

2.3.1 Discretization method **10**

2.3.1 ARMAX (Autoregressive Moving Average with exogenous inputs) **11**

2.4 TREMOR EXTRACTION **13**

2.4.1 The convolutive mixtures model **13**

2.4.2 Deflation method **14**

3.0 IDENTIFICATION AND QUANTIFICATION 16

3.1 Intrinsic Stiffness Dynamics 16

3.2 Reflexive Delay 19

3.3 Identification Procedure For Stretch Reflex Contribution 20

3.4 Tremor Quantification 21

4.0 RESULTS 22

4.1 Data Preparation 22

4.2 Reflexive Delay 23

4.3 Intrinsic Stiffness 25

4.4 Reflex Stiffness Contribution 31

4.5 Parkinson's Disease Tremor 32

5.0 DISCUSSION AND CONCLUSIONS 35

5.1 Discussion 35

5.2 Conclusions 38

BIBLIOGRAPHY 39

LIST OF TABLES

Table 1: Table of Reflexive Delays 24

Table 2: Intrinsic stiffness dynamics 31

LIST OF FIGURES

Figure 1: Test Apparatus..... 5

Figure 2: Pseudo Random Binary Signal (PRBS) 6

Figure 3: Parallel pathway model for joint stiffness..... 8

Figure 4: The ARMAX model. 12

Figure 5: Convolutive mixture model..... 14

Figure 6: EMG. 19

Figure 7: Joint Angle, Torque and Velocity signals..... 23

Figure 8: Position perturbation and corresponding EMG peak 24

Figure 9: Perturbation and corresponding torque response (poor fit)..... 25

Figure 10: Perturbation and corresponding torque response (improved steady state fit). 28

Figure 11: Reduction of Bias 29

Figure 12: Intrinsic Torque estimate 30

Figure 13: Intrinsic and Reflex stiffness Torque contributions. 32

Figure 14: EMG sources and spectral analysis 33

Figure 15: BSSD sources and spectral analysis..... 34

ACKNOWLEDGEMENTS

I would like to thank all people who have helped and inspired me during my thesis.

I especially want to thank my advisor, Dr. Zhi-hong Mao, for his guidance during my research and study at University of Pittsburgh. His perpetual energy and enthusiasm in research had motivated all his students, including me. In addition, he was always accessible and willing to help his students with their research. As a result, research life became smooth and rewarding for me.

I would like to extend my deepest gratitude to Dr. Xia, Neurologist department of Physical Therapy, Creighton University, who was abundantly helpful in providing experimental data, and has assisted us in numerous ways. Without her help and guidance this work would not have been possible.

I would also like to thank all my lab mates at the University of Pittsburgh who made it a convivial place to work. In particular, I would like to thank Ramana Vinjamuri, Robert O'Connor and Mircea Lupu for their friendship and help in the course of my work.

1.0 INTRODUCTION

‘Stiffness’ is defined as the ratio of steady force acting on a deformable elastic medium to the resulting displacement. This characteristic of muscles and springs is defined as the change in tension divided by the change in length. A very stiff spring requires a great deal of tension to increase its length [3]. Muscles behave in some ways like a spring. “The term 'Joint stiffness' indicates a dynamic relationship between the position of a joint and the torque acting about that joint, and consequently it plays a crucial role in the postural control in the face of perturbations. It is also vital in the control of movement, since it is the torque produced by the muscles that controls the final joint position” [4].

Pertinent scientific research has been carried out to investigate the joint stiffness of various joints of the human body including the shoulder [5], elbow [6] [7], and ankle [8]. Dynamic joint stiffness may be decomposed into two components namely intrinsic and reflexive components. [10]. The intrinsic stiffness component arises from the viscoelastic properties of the joint, passive tissue, and active muscle fibers. The reflex stiffness component arises from changes in the level of muscle activation due to afferent response to muscle stretch. The dependence of the muscle force on length and velocity is responsible for muscle stiffness and viscosity components. There is a second mechanism formed by reflex loops with muscle spindles afferent on muscle stretch and Golgi tendon organs afferent on active muscle force. En masse, the musculoskeletal system is a highly non-linear system, in which the arm dynamics depend on a combination of intrinsic muscle dynamics and reflexive feedback [5].

A trustworthy method for quantifying stretch reflex contributions to motor output would explicate the contributions of these reflexes during typical motor tasks in individuals with motor pathologies such as tremor, spasticity, and partial motor paralysis [11]. Until recently, reflex responses in intact, able-bodied human subjects could be studied only through the use of methods that eliminate reflex by effectively deafferenting a muscle [12], ischaemia [13] [15],

and using nerve blocks [16] or electrical stimulation [15] of the primary afferents. In spite of showing significance of reflex contributions under many conditions, these methods suffer from several limitations. These techniques involve physical disruption of the balance between a large number of descending and segmental inputs as a result of deafferentation and a corresponding change in the stretch response. Thus, these methods give just a crude picture of the reflex behavior [11].

More recently, system identification methods have been used to separate the intrinsic and reflex contributions analytically [8] [17] [18]. These methods use mathematical model approach to quantify the intrinsic and reflex dynamics of motor behavior using signal processing techniques and the known phenomena of 'Reflex delay' to separate reflexive contributions to motor output from intrinsic contributions.

Ancillary to quantifying stretch reflex contributions, one of the major problems faced by clinicians in evaluating movement disorders like Parkinson's disease (PD) is the quantification of Parkinsonian tremor to gauge the degree of severity of the disease. Tremor associated with Parkinson disease (PD) is one of the most widely studied and the second most common pathological tremor [19]. Presently, clinicians are relying on clinical rating scales such as Unified PD Rating Scale and Fahn-Tolosa-Marin (FTM) Tremor Rating Scale, which just quantify severity of tremor based on a 0-4 point system pertinent to daily activities or severity of resting and postural or kinetic tremor [20]. As the resolution of the scales is unknown, researchers are evaluating tremor based parameters like stiffness, rigidity, etc. [21] measured electro-mechanically. Also, it is virtually impossible to compare the results of clinical studies using a Tremor rating scale with those using motion transducers such as accelerometers and digitizing tablets.

Owing to its oscillatory characteristic, tremor is well suited to spectral analysis and time-frequency analysis [22] [23] [24]. However, applying spectral analysis methods directly might not result in the optimal quantification of tremor. This is because tremor is spread across parts of the limb and a single site of recording will not divulge significant tremor measurement. [21] Therefore in dissimilitude to previous methods, we take advantage of a technique involving blind source separation of convolutive mixtures to extract sources of tremor using surface EMG signals from the forearm.

Hence, the purpose of this work was twofold:

First; to apply parallel pathway joint stiffness model [8] to carry out system identification on the wrist joint for Parkinson's disease patients. This was realized by acquiring data through the use of a test setup designed for perturbation experiments on the joint, discretizing the continuous-time model in the parallel pathway stiffness model, performing ARMAX system identification technique to determine the models parameters, and realize the intrinsic and reflexive torque contributions.

Second; to quantify severity of tremor in Parkinson's disease patients. This was achieved by acquiring surface EMG data from six muscles of the forearm and using blind source separation technique followed by spectral analysis to extract and quantify tremor components.

2.0 ANALYSIS METHODS

2.1 TEST DESCRIPTION

2.1.1 Instrumentation

The test setup consists of an adjustable chair, forearm splint, and servomotor used to stretch and shorten wrist muscles by applying positional perturbations to the subject's wrist joint. The subject sits in an adjustable chair and places their hand into a U shaped channel which is connected to the servomotor, as depicted in Figure 1. The axis of the wrist joint is aligned with the shaft of the servomotor, so that rotation of the servomotors shaft produces an equivalent angular rotation of the wrist joint. The subjects arm is supported on a horizontal plane and secured in place using a vacuum bag splint to prevent forearm pronation and supination. This splint ensures that any torque measured will be purely from the flexor and extensor muscle groups that control the wrist joint.

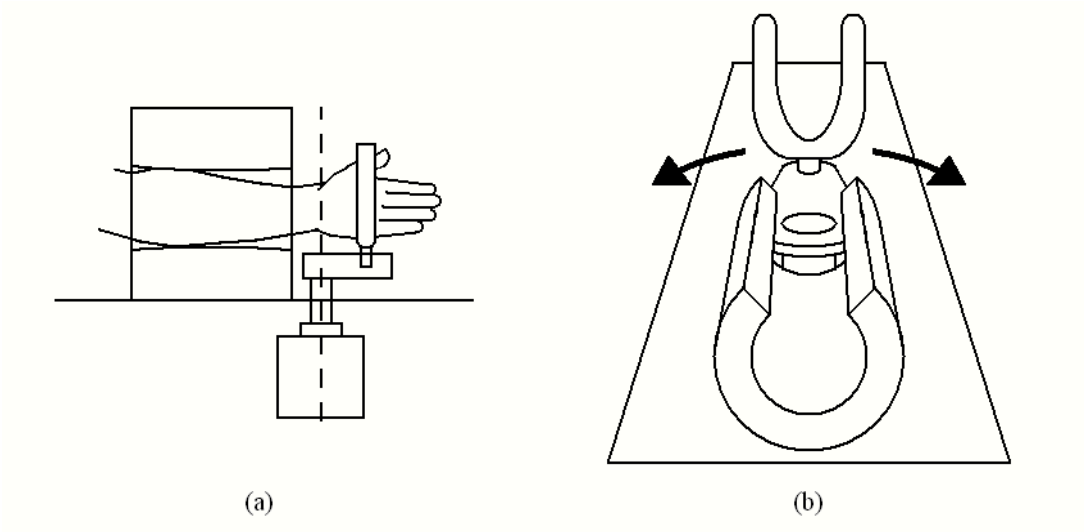

Figure 1: (a) Horizontal view of test apparatus (b) Top down view of test apparatus.
(Provided by Dr. Ruiping Xia, Neurologist, Creighton University)

2.1.2 Perturbation Signal Design

The servomotor is driven by a computer-generated pseudo-random binary sequence, as seen in Figure 2. The displacement amplitude was 2.5 degrees in both directions. It is important that the positional rotations must be small enough to linearize the joint stiffness characteristics, but large enough so that stiction of the wrist joint is a small contributor to the dynamic response.

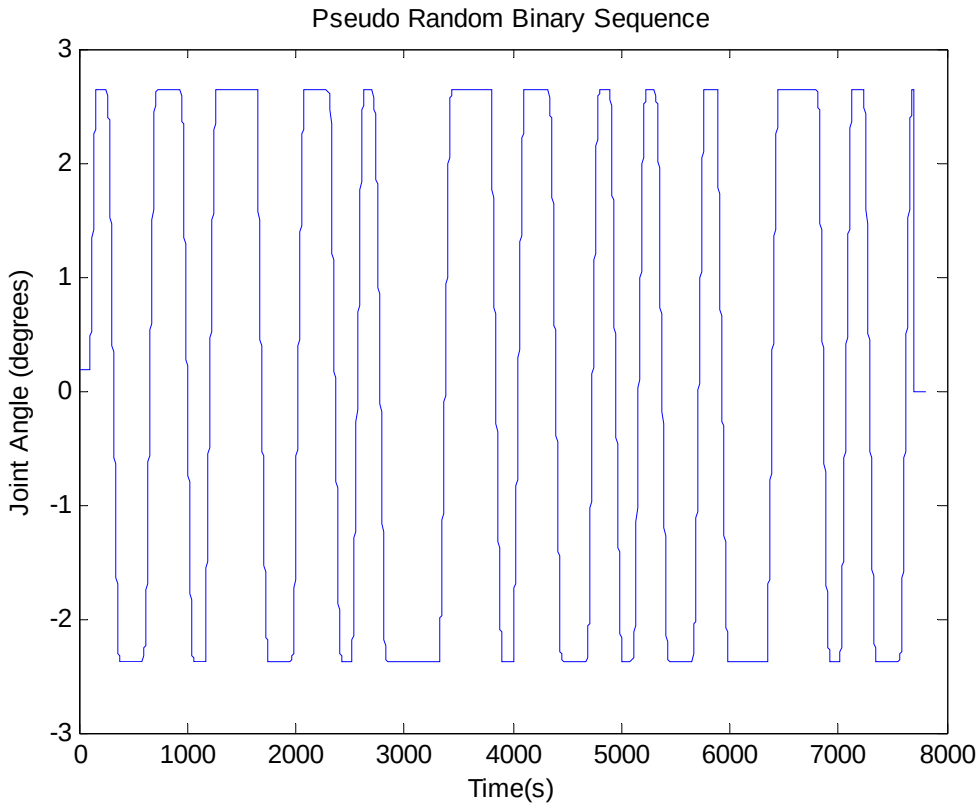

Figure 2: Sample Pseudo Random Binary Signal (PRBS) position change.
(Provided by Dr. Ruiping Xia, Neurologist, Creighton University)

2.1.3 Test Subjects

Four test subjects were recruited and referred by Dr. Ruiping Xia, Neurologist department of Physical Therapy, Creighton University. These subjects experienced joint rigidity as a predominant symptom of Parkinson's disease. Prior to testing, the subjects were rated for severity of disability and rigidity on the unified Parkinson's disease rating scale (UPDRS) by means of a motor examination. All subjects had consented to the experiment which was approved by the Institutional Review Board of Creighton University.

2.1.4 Testing Protocol

Test subjects were asked to be seated in a chair whose height was adjusted until their forearm rested comfortably on the arm splint. Before starting the test, a neutral position, defined as zero degrees, was found by both visual alignment and passive force measurement. Next, test subjects were given practice trials to become accustomed to the device. There was a two-minute break to prevent fatigue and avoid potential habituation. Each subject was asked to completely relax the wrist muscles to their maximum capability and then the pseudo-random binary sequence was applied. To preclude a test subject from predicting a forthcoming perturbation through habituation and thus preparing a reflexive resistance before it occurs, a pseudo random sequence was used. Thus, prediction of a perturbation was not possible during these tests due to the pseudo-random nature in which the perturbation signal was generated.

Surface EMG signals were recorded from the Flexor Carpi Radialis (FCR), Flexor Carpi Ulnaris (FCU), Extensor Carpi Radialis (ECR), Extensor Carpi Ulnaris (ECU), Flexor digitorum superficialis muscle, and Extensor digitorum (communis) muscles using differential surface electrodes. The EMG signals were amplified by 10 and band-pass filtered with a bandwidth 20 - 450 Hz before sampling at a rate of 1 kHz per channel. The area where the electrodes were applied was properly prepared and the electrodes were placed over the belly of each muscle. Angular position and velocity were recorded using the encoder outputs from the servomotor controller. Joint torque was measured with a strain gauge torque transducer. The angular position, velocity, and joint torque were sampled at 1 kHz per channel. (Note: All data recorded and provided by Dr. Ruiping Xia, Neurologist, Creighton University)

2.2 PARALLEL WRIST STIFFNESS DYNAMICS

The stretch reflex contributions to motor control comprising of intrinsic and reflex components can be analytically realized as a parallel pathway stiffness model as shown in Figure 3 [8]. Similar model has been used to study stiffness characteristics of the ankle [8], shoulder [5], and elbow [6] [7] joints. In spite of the differences in the movements of these joints from that of the

wrist, it has been propounded that this model is quite robust and efficient [10] and the same model can be used for the joint under consideration owing to the parallelism in their mechanical, muscular and neural properties [2].

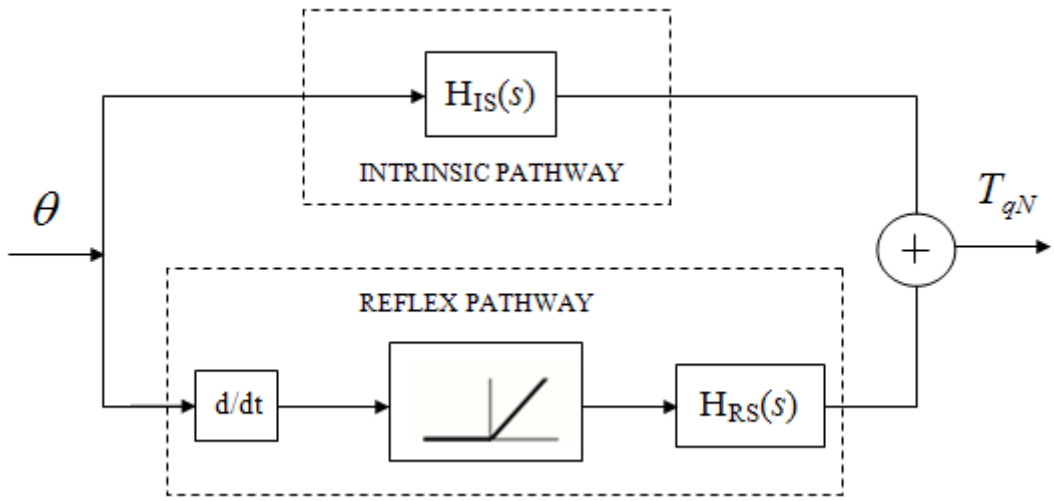

Figure 3: Parallel pathway model for joint stiffness.

2.2.1 Intrinsic Stiffness

Intrinsic stiffness is a passive component of joint stiffness pertinent to the viscoelastic joint properties. Movement disorders including Parkinson's disease that affect the central nervous system theoretically should not have an effect on any of the intrinsic stiffness parameters. "However, factors such as age, past injuries and diseases that affect the tissues that act as cushions inside the joints such as Osteoarthritis and Rheumatoid arthritis can have an effect on these parameters; therefore, patients in the study were screened for these conditions" [2]. The intrinsic torque component is due to the force required to overcome the mechanical properties of the joint. These intrinsic properties of muscles are arbitrated by the force-length and force-velocity characteristics of a muscle and are dependent on the motorneuron commands generated above the

spine [5]. The intrinsic pathway is modeled as a linear pathway subsuming inertial, viscous and elastic constituents and no delay [8]. The Intrinsic stiffness dynamics can be represented by the following second order equation,

$$H_{IS}(s) = \frac{T_{qI}(s)}{\theta(s)} = Is^2 + Bs + K \tag{2.2}$$

where T_{qI} is intrinsic torque, θ is joint angle relative to the rest reference position, I is inertial parameter, B is viscous damping parameter, K is elastic stiffness parameter and s is Laplace variable. K is also considered as the steady state gain of the system described in above equation owing to the frequency dependency of the Laplace variable s.

2.2.2 Reflexive Stiffness

The reflexive torque component is thought of as a force in response for overcoming a rotational perturbation. As Parkinson's disease causes chemical imbalance in brain affecting the central nervous system which therefore affects motor control, reflexive stiffness is expected to be affected by this disease [2].

The reflexive component is modeled as a velocity sensitive pathway subsuming a delay, a static nonlinearity that resembles a half wave rectifier, and then a dynamic linear element which is a low pass filter [8]. The static nonlinearity is a half wave rectifier since flexion and extension muscle systems are different. Both systems though characterized by the same model operate on different groups of mucles. Flexion motions target the Flexor/Pronator group of muscles including the Flexor carpi radialis, Palmaris longus, and Flexor carpi ulnaris, while extension motions target the Extensor/Supinator group including the Extensor carpi radialis brevis, Extensor carpi radialis longus Extensor carpi ulnaris. These muscles are different anatomically and thus have different gain, damping and natural frequency [2].

The linear element dynamics of reflexive stiffness can be modeled as a standard second-order low-pass system in series with a delay element as,

$$H_{RS}(s) = \frac{T_{qR}(s)}{V(s)} = \frac{G_R \omega_0^{\ 2}}{s^2 + 2\xi\omega_0 s + \omega_0^{\ 2}} e^{-st} \tag{2.3}$$

where T_{qR} is reflexive torque, V is joint angular velocity, G_R is the reflexive gain, ω_0 is the natural frequency, ξ is the damping factor, t is the reflex delay, and s is the Laplace variable.

2.2.3 Reflexive Component Delay

Reflex is defined as the change in muscle activation in response to an external perturbation thereby leading to a change in force. The Reflex pathway or the reflexive system may be viewed as a feedback control system that acts for stabilization. When the wrist position is rapidly perturbed, the neuromuscular reflex response changes the muscle activations to attempt to reject it and return the system to its original configuration. The Reflex delay attributes to the time from the perturbation to the onset of reflex activation. In case of simple movements, like the ones in this experiment, the spinal cord is adept enough to systematize muscle activity without the help of the brain which is only necessary for complex or atypical motions [2]. Quantification of this delay is imperative in order to accurately quantify the intrinsic torque component and subsequently the reflexive torque component.

2.3 PARAMETRIC ESTIMATION

2.3.1 Discretization method

The bilinear transform is a first-order approximation of the natural logarithm function that is an exact mapping of the z-plane to the s-plane. The bilinear transform maps the left half of the complex s-plane to the interior of the unit disc and the imaginary axis on the circumference of the unit disc in the z-plane. Thus filters designed in the continuous-time domain that are stable are converted to filters in the discrete-time domain that preserve that stability [25]. Such a

complete mapping also means that the bilinear transform has a good characterization of the higher frequency components of a system [26].

The bilinear transform is

$$z = e^{sT}$$

$$\Rightarrow s = \frac{1}{T}\ln(z) = \frac{2}{T}\left[\frac{z-1}{z+1} + \frac{1}{3}\left(\frac{z-1}{z+1}\right)^3 + \frac{1}{5}\left(\frac{z-1}{z+1}\right)^5 + \frac{1}{7}\left(\frac{z-1}{z+1}\right)^7 + \ldots\right]$$

$$\Rightarrow s = \frac{d}{dt} = \frac{2}{T}\frac{z-1}{z+1} = \frac{2}{T}\frac{1-z^{-1}}{1+z^{-1}} \tag{2.4}$$

where, s is the Laplace variable, T is the sampling time, and z is the shift operator for the z-domain.

2.3.1 ARMAX (Autoregressive Moving Average with exogenous inputs)

The ARMAX technique is a standard tool in control and econometrics for both system description and control design. Given a set of time series data, an ARMAX model is a technique for understanding and forecasting values of the time series. These models represent time series that are generated by passing white noise through a recursive and through a non-recursive linear filter, consecutively. In other words, the ARMA model is a combination of an autoregressive (AR) model and a moving average (MA) model, and combines linearly current and prior terms of a known, and external, time series [2] [27].

The autoregressive model describes a stochastic process that can be described by a weighted sum of its previous values combined with a white noise error signal [28]. This means that a value at time t is based upon a linear combination of prior and current values of the output. The moving average part is used as a low-pass filter in order to smooth out the time series and reduce some of the high-frequency variance, thus highlighting long-time trends [28].

It is not possible to identify time-varying parameters using this model, therefore, the parameters are assumed to have stationary distribution within the time series being examined. Time-varying parameters can be estimated by using a recursive identification method, but in the

case of the wrist stiffness model, the parameters are considered stationary. It is possible that fatigue could affect the parameters over time [2], but the testing duration is short and test subjects are given long breaks between tests to reduce the potential for fatigue issues.

The following figure describes the ARMAX model structure:

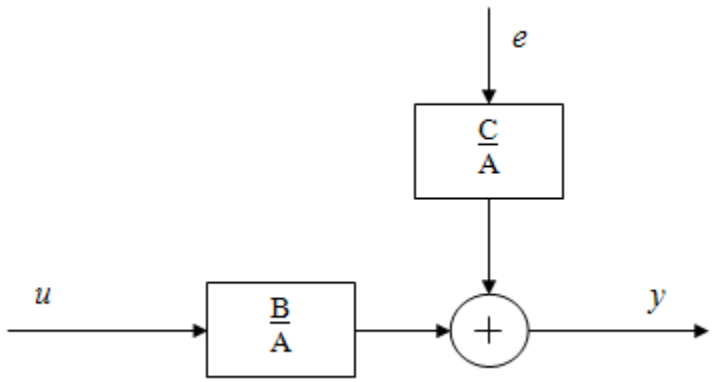

Figure 4: The ARMAX model structure.

Thus, the general form of an ARMAX model is: [27]

$$Ay(t) = Bu(t) + Ce(t) \tag{2.5}$$

The above form indicates the I/O relationship of a linear system written in the form of a difference equation where y is the output, u is the exogenous input and e is an uncontrolled input, such as white noise. A, B, and C are polynomials in z whose orders represent the orders of the models. The higher the order of these polynomials, the more prior values of the time series are necessary.

After specifying the orders, least squares regression is used to find the coefficients of the polynomials in order to minimize the prediction error. For the k-*th* entry in the time series, prediction error is defined as,

$$\varepsilon(k,\theta) = y(k) - \hat{y}(k) = y(k) - \phi(k)^T \theta \tag{2.6}$$

where, $\phi(k)$ contains lagged input and output variables, θ is the parameter vector, y is the actual output of the system, and $\hat{y}$ is the estimated output.

In system identification, one of the best estimates of parameters will yield the minimum of the sum of the squared prediction error [27]. The least squares criterion for the linear regression can be written as,

$$V_N(\theta, Z^N) = \frac{1}{N}\sum_{k=1}^{N} \tfrac{1}{2}\left[y(k) - \phi(k)^T\theta\right]^2 \tag{2.7}$$

where, $Z^N = \left[y(1), u(1), y(2), u(2), ..., y(N), u(N)\right]$ is the batch of data collected from the system.

The unique feature of this criterion is that it is quadratic in θ. Therefore, it can be minimized analytically, which gives the least squared estimates,

$$\hat{\theta}_N^{LS} = \arg\min V_N(\theta, Z^N) = \left[\frac{1}{N}\sum_{k=1}^{N}\phi(k)\phi(k)^T\right]^{-1}\frac{1}{N}\sum_{t=1}^{N}\phi(k)y(k) \tag{2.8}$$

Provided the inverse exists.

2.4 TREMOR EXTRACTION

2.4.1 The convolutive mixtures model

The convolutive mixtures model treats the recorded EMG signals believed to contain tremor, as convolutive mixtures of source signals created in the higher level neural system. This can be seen in the Figure 5.

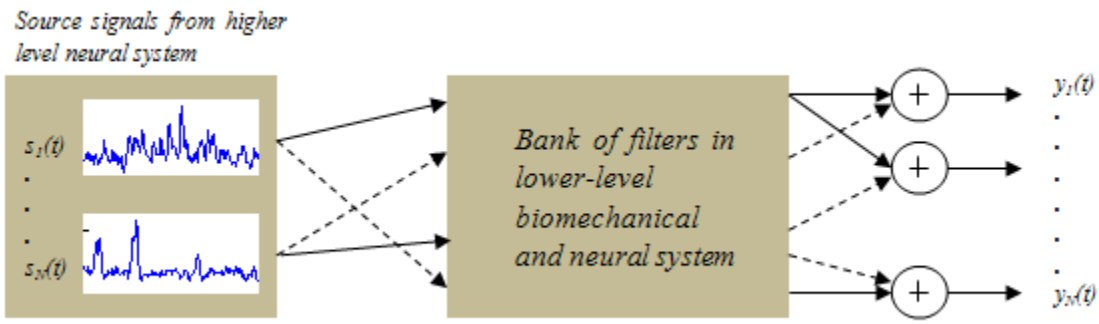

Figure 5: Convolutive mixture model of signals originating in higher level neural system and going through filters in lower level biomechanical and neural system. (Fig. adapted from [21])

In the model, an impulse originating in the higher level neural system activates some mechanisms in the lower level neural system, followed by the simulation of certain biomechanical structures to finally create a movement about the joint. These phenomena can be simplistically attributed to the production of impulse responses by filters [21]. The assumption made is that all the filters have finite impulse responses and are linear. This assumption is made on the fact that even though the neuromuscular system is nonlinear, making a linear approximation can provide a useful insight of the system.

The convolutive mixture model can be expressed by the following equation:

$$\forall n, \qquad x_i(n) = \sum_j h_{ij} * s_j(n) \tag{2.9}$$

where $x(n) = [x_1(n), \ldots\ldots\ldots, x_Q(n)]^T$ is the observation vector; $s(n) = [s_1(n), \ldots\ldots\ldots, s_N(n)]^T$ is the source vector; and h_{ij} is the impulse responses matrix of the mixing filters with N inputs and Q outputs.

2.4.2 Deflation method

We use the model in Eq. (2.9) to extract sources of tremor from recorded EMG signals of PD patients. An algorithm for blind source separation [29] through deflation is used to realize the

same [21]. The algorithm executes blind source separation in an iterative manner using kurtosis real-valued contrast of cumulants. Kurtosis is a quantity that signifies Gaussianity or non-Gaussianity in signals which is used to indicate independence [30] of signals. The kurtosis of a normalized random variable y, where $E\{y\} = 0$ and $E\{y^2\} = 1$, is defined by,

$$E\{y^4\} - 3\left(E\{y^2\}\right)^2 = E\{y^4\} - 3 \tag{2.10}$$

The kurtosis contrast function used in the algorithm facilitates the extraction of one non-Gaussian or independent source at a time from the mixture. Subsequent to its extraction, the contribution of the extracted source is then subtracted from the observations.

This process is known as 'deflation' and is used to extract all the sources from the observation signals. The use of filters having finite response reduces the problem to a least squared linear regression problem [29].

3.0 IDENTIFICATION AND QUANTIFICATION

3.1 INTRINSIC STIFFNESS DYNAMICS

The model concerning the intrinsic pathway or the intrinsic stiffness component was described in Eq. (2.2). However, the system identification of such a model's parameters becomes problematic since its lack of poles causes instability at high frequencies thus exhibiting an unbounded response. Therefore, it is advisable to use the dynamic inverse of the intrinsic stiffness model instead [8] which results in the equation,

$$H_{IC}(s) = \frac{\theta(s)}{T_{qI}(s)} = \frac{1}{Is^2 + Bs + K} \tag{3.1}$$

This is known as the intrinsic compliance model and resembles the well known Mass-Spring-Damper System where I is the mass, B is the coefficient of viscous damping parameter and K is the spring stiffness. When the intrinsic stiffness dynamics are discretized using Tustin's approximation, the intrinsic stiffness dynamics become,

$$H(z) = \frac{\theta(z)}{T_{qI}(z)} = \frac{1 + 2z^{-1} + z^{-2}}{\left(\frac{4I}{T^2} + \frac{2B}{T} + K\right) + \left(\frac{-8I}{T^2} + 2K\right)z^{-1} + \left(\frac{4I}{T^2} - \frac{2B}{T} + K\right)z^{-2}} \tag{3.2}$$

The above equation is nothing but an Auto regressive moving average filter. Due to the presence of a reflex delay, it can be assumed that from the beginning of a rotational displacement perturbation and up until the torque response occurs, the torque is purely due to the intrinsic stiffness dynamics. In most cases, despite of the reflexive delay being accurate it is only

considered as an estimate [2]. It is known that the first 40 ms of response to a perturbation is purely intrinsic [8] and, knowing that the intrinsic dynamics can be modeled as a FIR filter of the second order, the system response should have occurred within this 40 ms period. Consequently, an accurate identification of the intrinsic system is possible. Therefore, only the first 40 ms of torque response after a perturbation occurs is used in the identification procedure to determine the intrinsic compliance dynamics.

Before carrying out the ARMAX identification, we need to carry out some mathematical adjustment to force the numerator of the discretized intrinsic compliance transfer function to 1, so that the ARMAX identification and subsequent parameter identification viz. of I, B, and K is more accurate.

To do this, we filter the torque signal through a filter whose weights are the coefficients of the numerator in the discretized transfer function thus yielding a new intermediate torque signal T_{qI_new} in order to carry out ARMAX identification. This process is shown below:

$$\frac{\theta(z)}{T_{qI}(z)} = \frac{1+2z^{-1}+z^{-2}}{\left(\frac{4I}{T^2}+\frac{2B}{T}+K\right)+\left(\frac{-8I}{T^2}+2K\right)z^{-1}+\left(\frac{4I}{T^2}-\frac{2B}{T}+K\right)z^{-2}} \tag{3.3}$$

$$T_{qI\_new} = T_{qI}(z)(1+2z^{-1}+z^{-2}) \tag{3.4}$$

$$\frac{\theta(z)}{T_{qI\_new}(z)} = \frac{1}{\left(\frac{4I}{T^2}+\frac{2B}{T}+K\right)+\left(\frac{-8I}{T^2}+2K\right)z^{-1}+\left(\frac{4I}{T^2}-\frac{2B}{T}+K\right)z^{-2}} \tag{3.5}$$

The ARMAX identification procedure is an iterative search algorithm which minimizes a robustified quadratic prediction error criterion using Gauss-Newton approach or Levenberg-Marquardt method. It is used to obtain an initial estimate of the intrinsic torque. Using this estimate, the ARMAX identification procedure is performed on the entire data set to find the proper order I/O relationship of the form,

$$\frac{\theta(z)}{T_{qI\_new}(z)} = \frac{1}{a_0 + a_1 z^{-1} + a_2 z^{-2}} \tag{3.6}$$

Relating Eq. (3.5) and Eq. (3.6) and using linear algebra, it is possible to find the relationship between the discrete-time and continuous time parameters:

$$\begin{bmatrix} a_2 \\ a_1 \\ a_0 \end{bmatrix} = \begin{bmatrix} \frac{4}{T^2} & -\frac{2}{T} & 1 \\ -\frac{8}{T^2} & 0 & 2 \\ \frac{4}{T^2} & \frac{2}{T} & 1 \end{bmatrix} \begin{bmatrix} I \\ B \\ K \end{bmatrix} \tag{3.7}$$

While performing ARMAX identification, we choose all the perturbation segments for a subject under test. Thus, at the end of the identification we have several sets of identified *I*, *B*, and *K* parameters which are further averaged to get a consistent set.

However, as further described in section 4.3, the above method does not yield good estimates. It was then decided to calculate the steady state gain *K* as follows,

$$K = \left. \frac{T_{qI}(s)}{\theta(s)} \right|_{s=0} \tag{3.8}$$

It was also found out that the original Torque response was delayed and had a peculiar bias value that prevented from accurate parameter estimation. The bias was eliminated using ‘Linear regression on the data to determine the bias parameter and the delay was taken care of by making use of the steady state gain from Eq. (3.8) and joint angle value. Further estimation of *I* and *B* parameters was carried out in a similar manner using Tustin’s discretization as described in this section.

3.2 REFLEXIVE DELAY

The Reflexive delay is defined to be the time between a change in rotational position of the wrist and a corresponding afferent response to the muscle perturbation. This response can be attributed to a spike in the EMG recorded from that muscle in response to the perturbation. Owing to the noisy characteristics of recorded EMG signals, a spike in the EMG is considered credible enough for characterizing the reflex delay only if it is above a threshold that is considerably greater than the variance of noise in the signal [2]. This threshold is set to be two standard deviations above the mean of the EMG signal under consideration. Figure 6 shows an example of such an EMG and the peaks located above the threshold relative to perturbations.

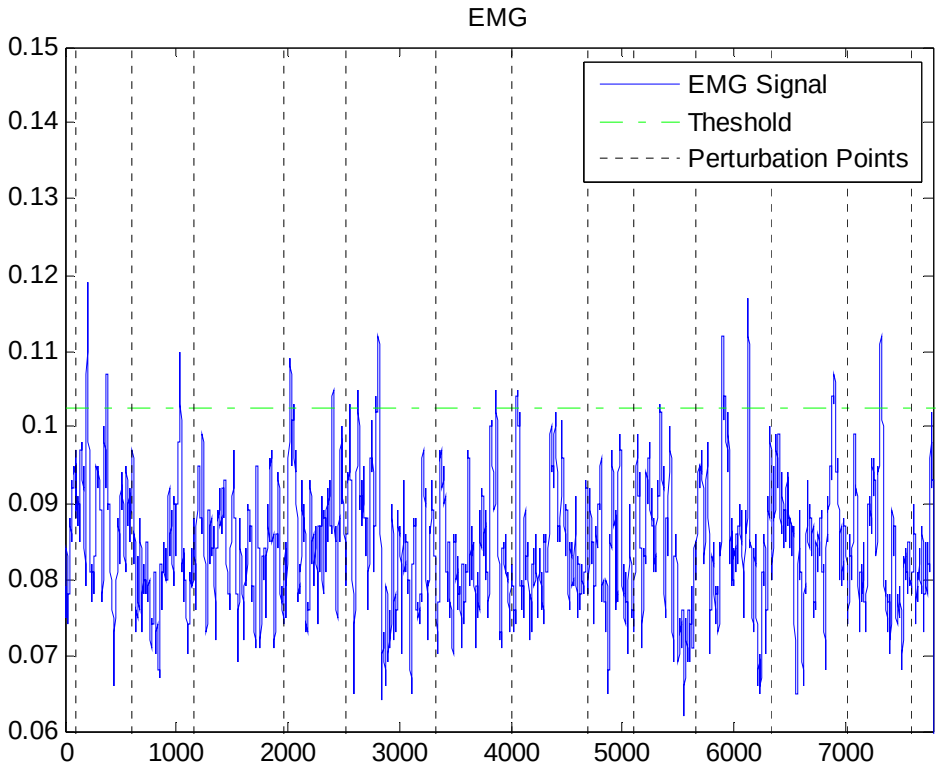

Figure 6: Typical EMG signal depicting significant peaks from each perturbation point above a set threshold.

Each muscle may not necessarily demonstrate a spike due to each perturbation in the position. Therefore, it is advisable to measure all the delays between the position signal and measured EMGs. The measured delays are then collected together and the final reflexive delay is considered to be the mean of all these delays after outlier removal.

The delay estimated from the above procedure is not necessarily the true delay. The identified peak in the EMG signal may not always indicate when the actual reflex occurred. It is ill-defined as to which part of the EMG spike the reflex actually takes place. Therefore, it is necessary to test a range of delays spanning from before to after the calculated delay. The delay that yields the best results pertaining to data-fits will be assumed to be the appropriate delay. Typical delay values range from 40ms to 50 ms of which we consider 40ms as a safe measure for identification.

3.3 IDENTIFICATION PROCEDURE FOR STRETCH REFLEX CONTRIBUTION

The parameter identification procedure is outlined below:

1. The reflexive component delay estimate is determined using the position and EMG data according to the methods of section 3.2.

2. Parameters for the intrinsic stiffness model are then calculated, as outlined in section 3.1, and an intrinsic torque estimate is calculated, $\hat{T}_{qI}$

3. Using the reflexive delay and intrinsic torque estimates, one can separate reflexive torque from the net torque,

$$\hat{T}_{qR} = T_{qN} - \hat{T}_{qI}$$

4. The predicted stretch reflex contributions calculated from the identified parameters are then plotted together to signify their contributions.

3.4 TREMOR QUANTIFICATION

The recorded surface EMG signals were used for tremor quantification. Initially, Fourier transforms were calculated for each EMG signal and after careful observation of both the EMG signals and their corresponding FFTs, three out of six signals were picked for further tremor source separation. This was done to avoid unnecessary averaging over the other sources depicting miniscule tremor activity so that only observations which contribute significantly to tremor can be treated. Note that the muscles from which the three signals were selected were different for different subjects.

The selected signals were then processed using an algorithm for blind source separation of convolutive mixtures by deflation method (BSSD toolbox provided by Castella *et al*.) [29]. We chose 'Kurtosis real valued' contrast function as the separation method for the algorithm [21]. Various filter lengths were considered and implemented and the best observed length was used with the algorithm to reveal tremor sources.

After extraction using BSSD algorithm, the extracted source signals believed to embody tremor were further analyzed by using Fast Fourier transform and short time Fourier transform based Time frequency analysis techniques. For comparisons, Time frequency analysis was also performed on the raw EMG data. A Hamming window of length 512 was used with the short time Fourier transform algorithm for Time frequency analysis.

4.0 RESULTS

4.1 DATA PREPARATION

It has been propounded that there are no significant frequency components in the torque signal obtained from the experimental data [8]. Hence, all the recorded data was filtered at a cutoff frequency of 100 Hz using an 8th order Butterworth filter to attenuate high frequency noise and was then re-sampled, implementing an anti-aliasing filter, at 200 Hz. All data was filtered using the same filter to ensure that the group delay, the sample delay induced by the filter, be the same for all signals. Figure 7 shows a grouping of the typical signals collected during an experiment including joint angle, joint velocity, and joint torque.

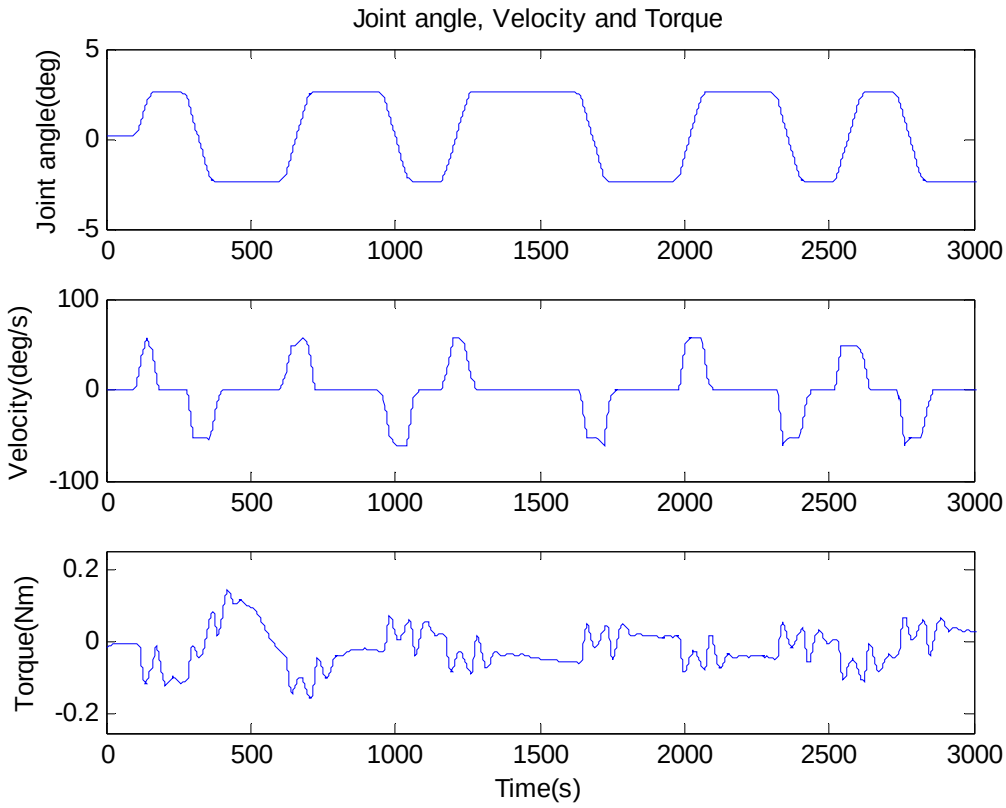

Figure 7: Typical Joint Angle, Torque and Velocity signals recorded from experiments

4.2 REFLEXIVE DELAY

The reflexive delay is, as it pertains to this test, the time it takes the afferent nerves to register a position change, send the signal up to your spinal cord and return a response signal to the muscle for actions. It was measured to be the time between a position change and a significant peak in the EMG signal as described earlier in section 3.2. Table 1 shows the results for the reflexive delay associated with each test subject. Some error is expected due to the band-pass filtering of the EMG signals as outlined in section 2.1.3. However, as mentioned in section 3.2, delays before and after these values were tested to eliminate this error. An example for a position change and a corresponding spike can be seen in the EMG in Figure 8, the time difference was measured as the delay.

Table 1: Table of Reflexive Delays

Test Subject	Delay (ms)
1	50.60
2	42.36
3	44.36
4	47.88

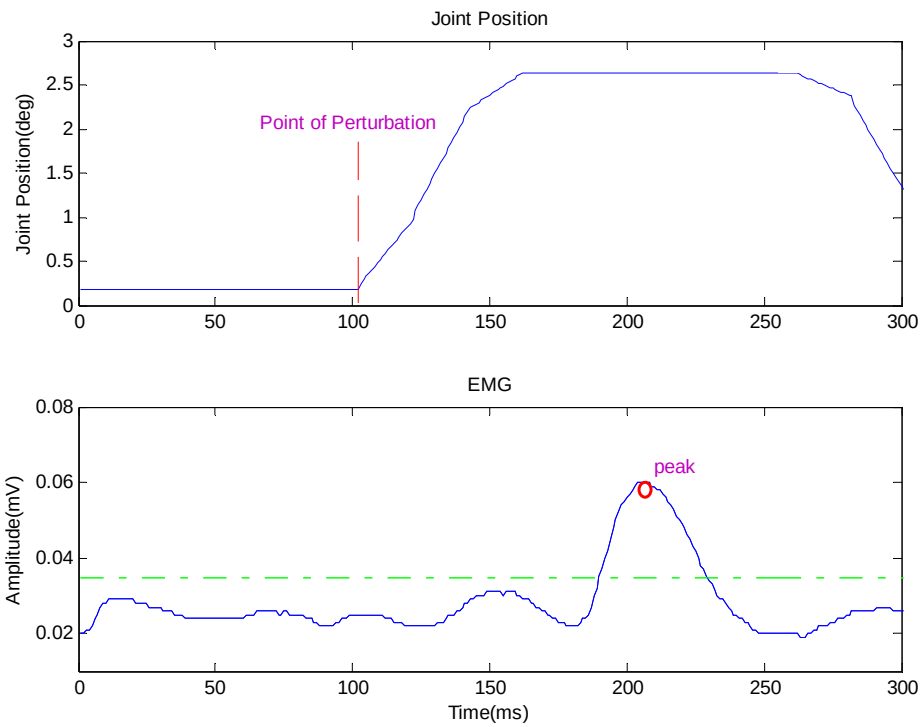

Figure 8: Position perturbation and corresponding EMG peak

4.3 INTRINSIC STIFFNESS

As discussed in section 3.1, we used Eq. (3.2) to determine intrinsic stiffness dynamics and obtain an estimate of the intrinsic torque response in correspondence to the total torque. It immediately became clear that this method did not yield satisfactory parameters and subsequently, unacceptable intrinsic torque estimates with a fit accuracy of less than 60% as is evident in Figure 9.

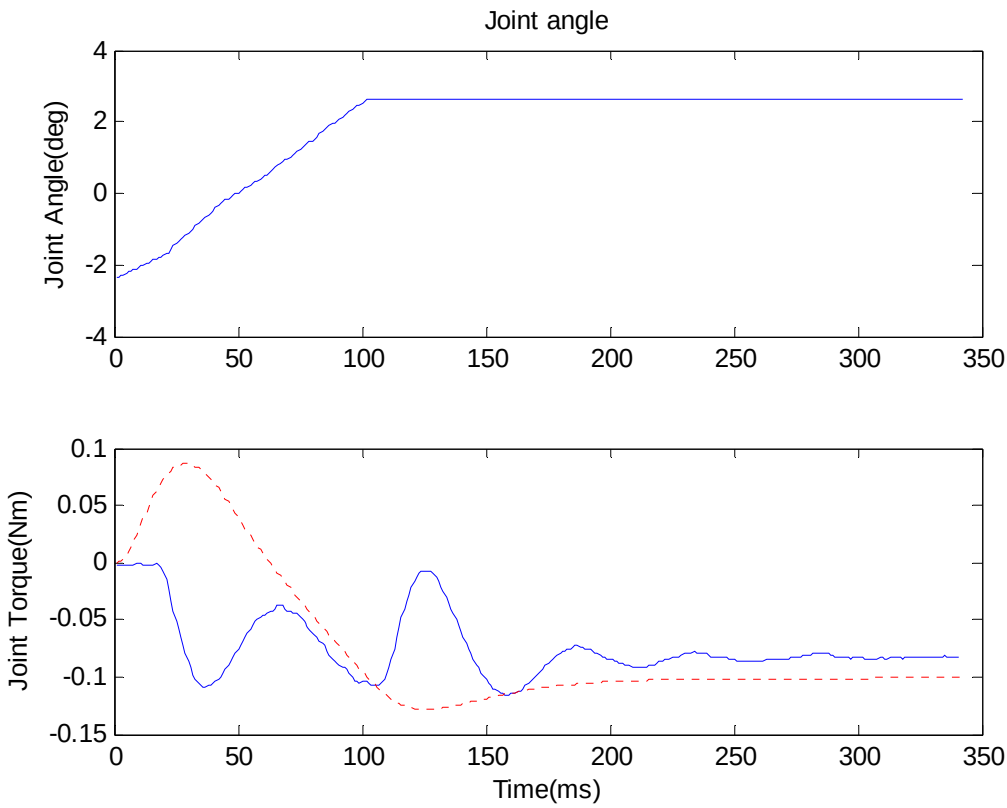

Figure 9: Joint position perturbation and corresponding torque response depicting a poor fit of the discretized intrinsic stiffness model.

As seen from Figure 9, the parameter estimates did not give a matching initial response curve based on the hypothesis that for the amount of the reflex delay there would be only passive contribution to the torque or in other words, only the intrinsic response would contribute to the total torque. Another unsatisfactory aspect of the above response was that it did not yield a good

steady state fit either. This meant that even the steady state parameter estimate yielded by this procedure was erroneous.

For this reason, it was decided to calculate the model's steady state gain K by computing the ratio of the steady state Joint position and Torque when s=0.

$$K = \left. \frac{T_{qI}(s)}{\theta(s)} \right|_{s=0} \tag{4.1}$$

This implied that, after a joint perturbation, according to the second order nature of the intrinsic stiffness model, the intrinsic response would die out leaving only the intrinsic gain as the steady state gain.

After the steady state parameter calculations according to Eq. (4.1), we proceeded to calculate the remaining parameters in the following manner:

As, described earlier, the intrinsic stiffness model was,

$$\frac{T_{qI}(s)}{\theta(s)} = Is^2 + Bs + K \tag{4.2}$$

$$\frac{T_{qI}(s) - K\theta(s)}{\theta(s)} = Is^2 + Bs \tag{4.3}$$

Using the above Eq. (4.3), we calculate a new torque signal,

$$\frac{T_{new}(s)}{\theta(s)} = Is^2 + Bs \tag{4.4}$$

Further, a similar discretization was carried out on the system in Eq. (4.4) and the remaining intrinsic stiffness dynamics viz. I and B were estimated. However, the system so predicted had the disadvantage that it was not proper when we considered the transfer function from the intrinsic torque estimate to the input position sequence since it lacked poles. In order to make the system proper, we cascaded the system with a low-pass filter which had stable poles

with values much greater than the roots of the model. This was to improve the speed of response of the system. We used a fourth order low-pass filter to make the system proper. The resulting system was as follows:

$$\frac{T_{qI}(s)}{\theta(s)} = \frac{Is^2 + Bs + K}{\left(\frac{s}{z_1}+1\right)\left(\frac{s}{z_2}+1\right)\left(\frac{s}{z_3}+1\right)\left(\frac{s}{z_4}+1\right)} \tag{4.5}$$

However, as it turned out, we did not get satisfactory torque responses from the model which had all estimated I-B-K dynamics averaged together. This meant that some sets of I-B-K values were outliers. We therefore decided to analyze each set separately by carrying out the same stabilization procedure. After stabilization, we subjected the system to the position input sequences for a 40ms interval after each perturbation point. We obtained get good but not satisfactory intrinsic torque responses. Such a response is shown in Figure 10.

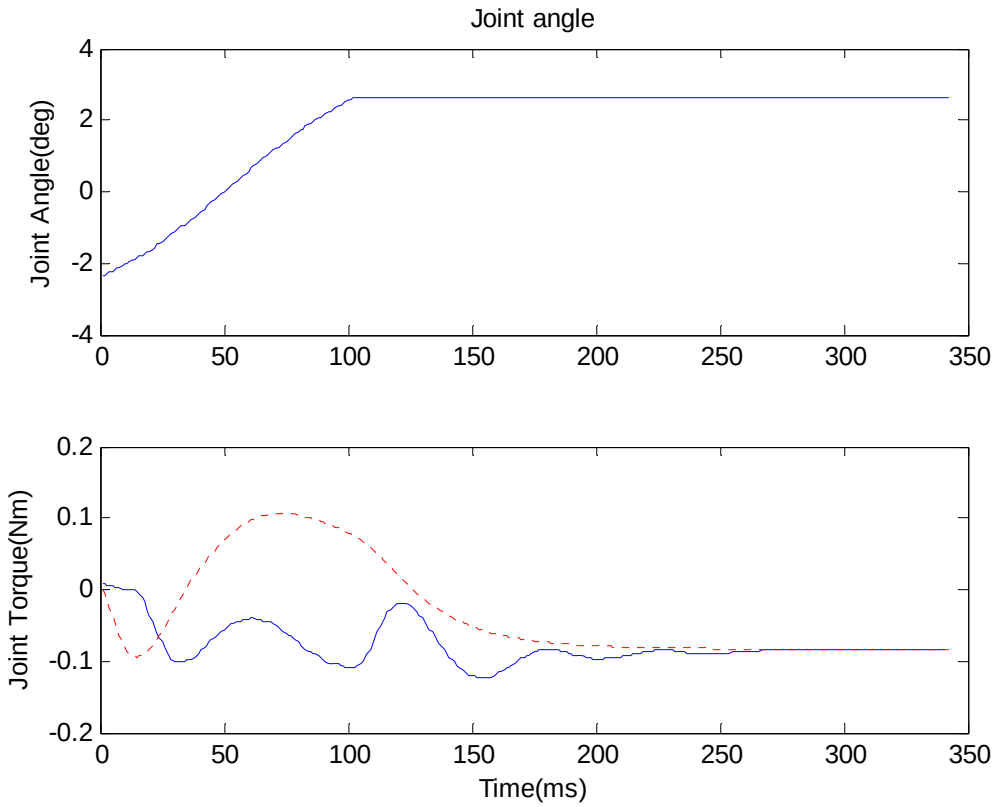

Figure 10: Joint position perturbation and corresponding torque response depicting an improved steady state fit for the model.

It was observed from the responses that there was a delay in the original torque signal from the point of perturbation. This delay was predicted using the criterion that before the start of each perturbation, the joint angle or the position value was constant. This meant that the Net Torque value at the start of each perturbation would solely be due to the product of steady state gain of the model i.e. due to the K value and joint angle θ.

Hence, the starting torque value for each perturbation set should be, $K.\theta$ where θ is the steady state joint angle value before the start value of each perturbation. The point where the Net Torque was closest to this product was considered to be the delay point and the Torque was advanced by the same amount before running it through for identification.

In addition to the delay, after observing the original recorded torque sequence, it was found that the recorded Torque contained a peculiar bias which was not giving proper results for system identification. In order to get rid of the bias, 'Linear regression' was carried out on the data using the following equation:

$$\tau - b_\tau = \theta \times k \tag{4.6}$$

Where, τ is the Torque, b_τ is the bias in the Torque, θ is the Position signal and k is a constant. Eq. (4.4) gave good value for the bias which is shown in Figure 11.

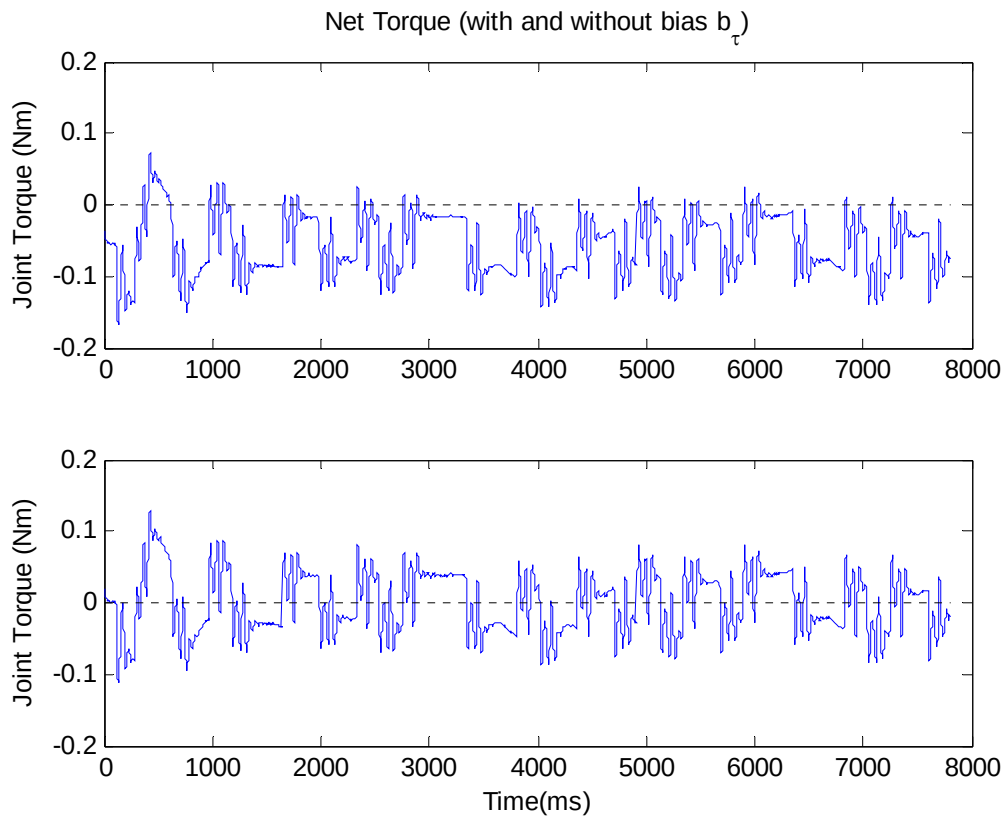

Figure 11: Reduction of inherent bias in Net Torque using 'Linear regression'

As seen from the above figures there was considerable bias in the torque signal which was reduced to form a new torque signal which was subsequently used for identification. Using this new torque signal and applying the method used in Eq. (4.5) further identification was carried out.

The parameter estimates found from this method proved to be very effective in extracting the intrinsic responses. It was found that all the intrinsic response estimates had a different starting value than the Net Torque, however, followed the Net Torque religiously after that. It

was determined that this difference in the start value was due to the effect of initial conditions in each perturbation dataset under consideration. Initial states were calculated from the 'State space' equivalents of the identified models. Then an initial state response was predicted and added along with the identified system prediction to give the final intrinsic response. The estimated intrinsic responses were considerably good for most of the perturbation sets. Some of the perturbation sets did not yield proper steady states which subsequently resulted in poor responses.

The final intrinsic torque estimates proved to be satisfactory which reflected on good identification of the model as well as incorporation of the effect due to initial conditions on the dataset under consideration. Such a response is shown in Figure 12.

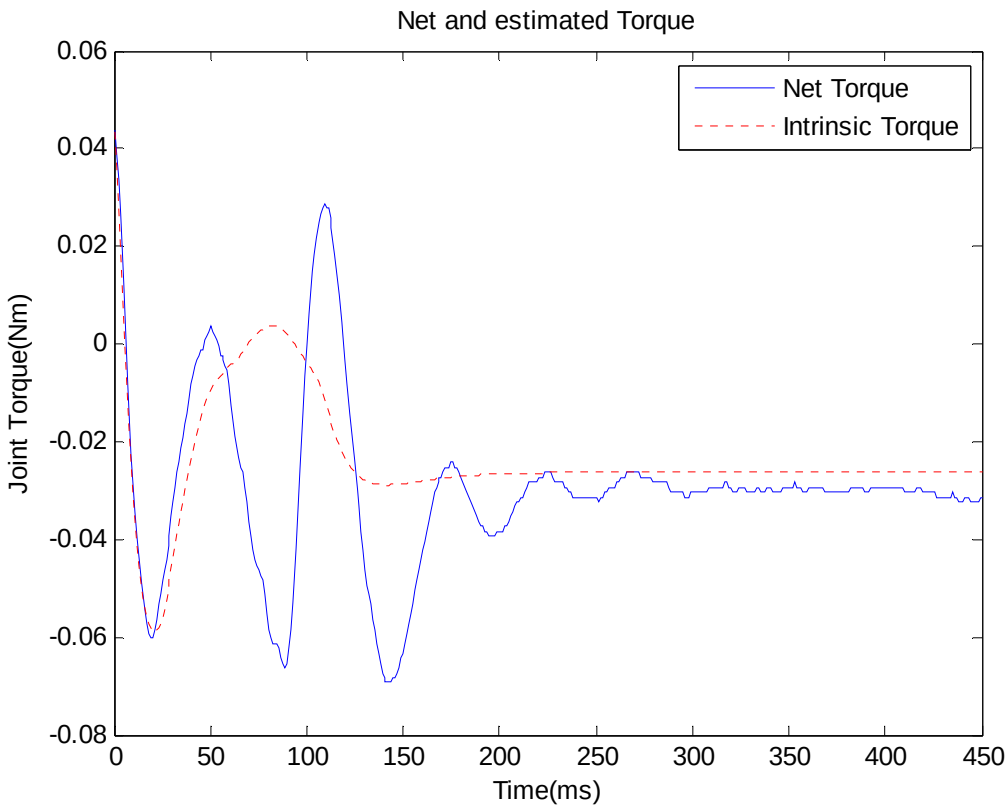

Figure 12: Intrinsic Torque estimate

4.4 REFLEX STIFFNESS CONTRIBUTION

After satisfactory intrinsic torque estimates were found out, the estimated model parameters yielding the best fits for respective perturbation datasets were selected and averaged to obtain single set of model parameters.

The following table shows the averaged IBK values for the data of 4 subjects:

Table 2: Intrinsic stiffness dynamics

Test Subject	*I (Nm/s^2/deg)*	*B (Nm/deg/s)*	*K (Nm/deg)*
1	11.8046e-006	148.3418e-006	9.9624e-003
2	25.6624e-006	400.7123e-006	11.7125e-003
3	306.8395e-009	1.4649e-003	15.5904e-003
4	11.0205e-006	1.2045e-003	15.6928e-003

After doing this, the reflex torque contributions were calculated by subtracting the intrinsic torque estimates from the Net Torque. The Reflex contribution can be seen in Figure 13.

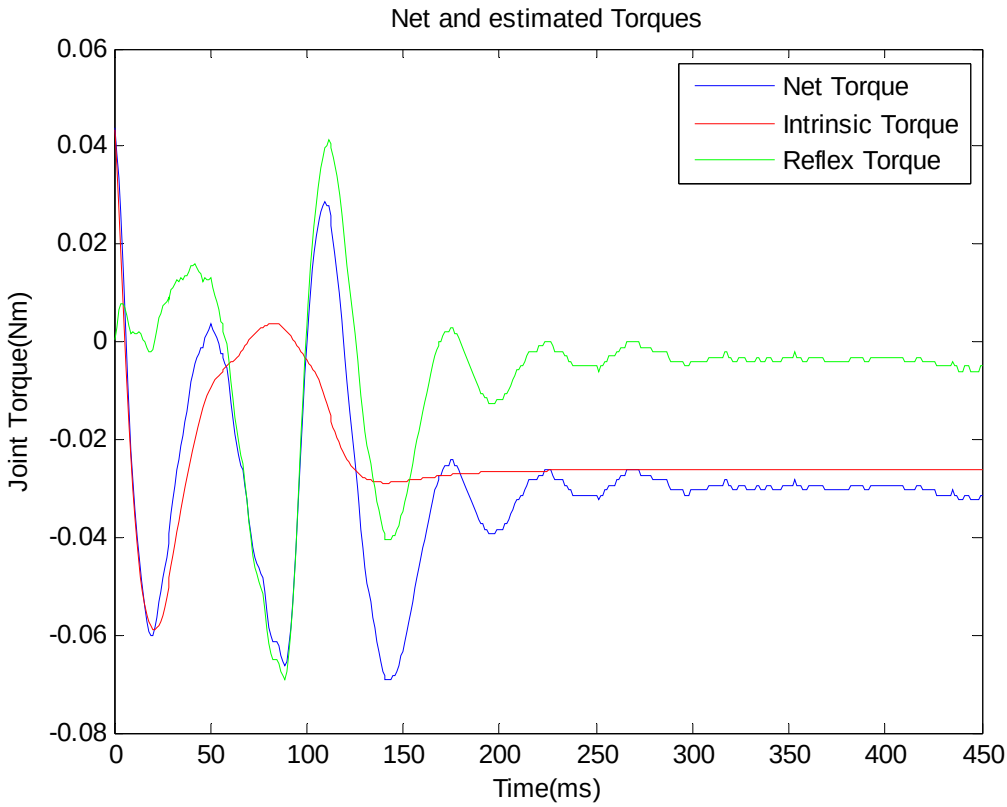

Figure 13: Intrinsic and Reflex stiffness Torque contributions.

It can be clearly seen from the figure that initially the 'Intrinsic Torque' follows the 'Net Torque' whereas; the 'Reflex' hovers around zero for the same time with a small value. After around 40ms, which is supposed to be the reflex delay, the 'Reflex Torque' follows the 'Net Torque' and the 'Intrinsic Torque' approaches steady state.

4.5 PARKINSON'S DISEASE TREMOR

The selected EMG signals exhibiting significant tremor activity were run through the algorithm of BSSD for convolutive mixtures. The filter lengths used during the deflation procedure ranged from 50-75. The most appropriate filter length for deflation and yielding satisfactory results was

found to be 75. The selected EMG signals for tremor separation, corresponding FFTs and their Time frequency analysis plots are shown in Figure 14.

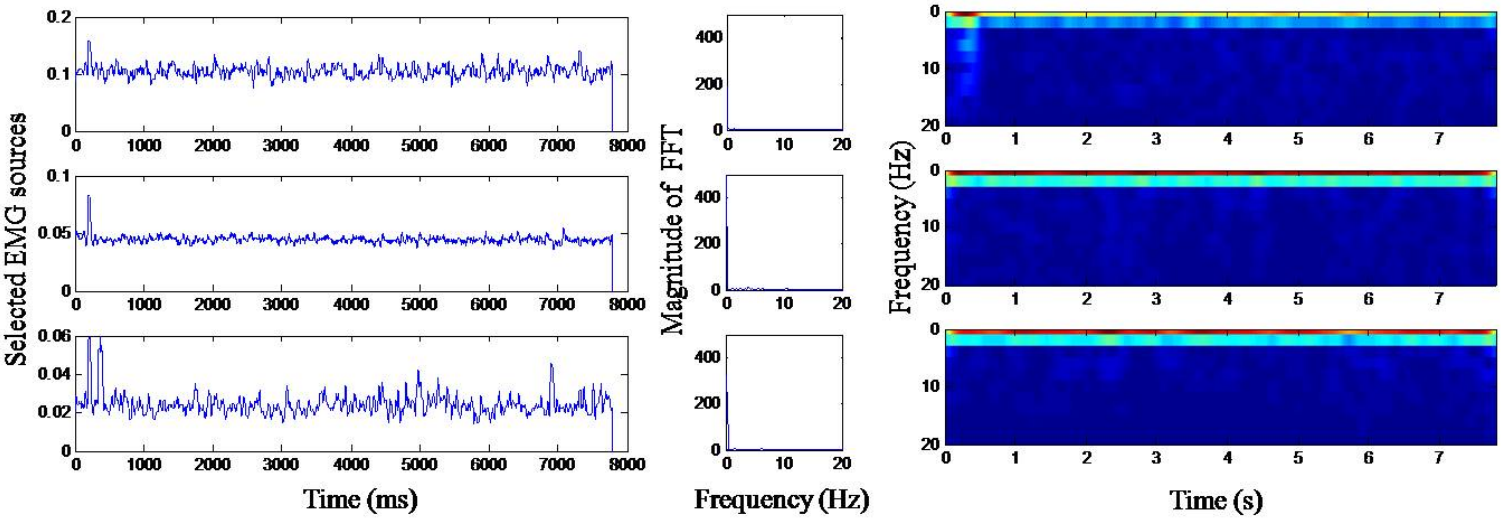

Figure 14: Selected EMG sources for Blind source separation (left), corresponding Fourier transforms (middle), and time-frequency spectra (right) [EMG data provided by Dr. Ruiping Xia, Neurologist, Creighton University]

The tremor components could be better appreciated for BSSD as opposed to direct spectral analysis on the raw EMG data. The extracted BSSD sources, corresponding FFTs and their Time frequency analysis plots are shown in Figure 15.

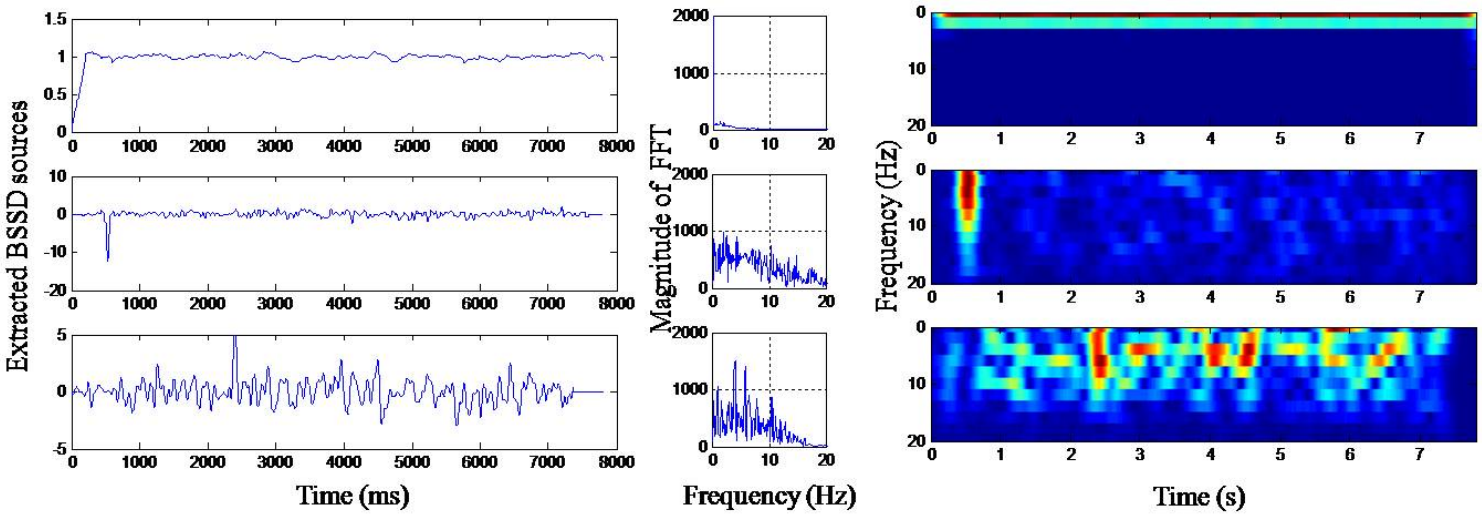

Figure 15: Sources extracted using Blind source separation (left), corresponding Fourier transforms (middle), and time-frequency spectra (right)

It can be clearly seen that the extracted BSSD sources revealed tremor peaks from 3-8Hz which were not visible in the spectral analysis of the selected raw EMG signals.

Though analysis of the frequency spectrum of the signals provided good measure and manifestation of tremor, it may be deceiving as the signals are assumed to be stationary. Therefore, in addition to spectral analysis, TFA was carried out for both the raw data and the extracted sources considering the signals as non-stationary [21]. It can be seen from the above figures that the TFA of the extracted source signals using BSSD outperformed TFA done directly on experimental recordings of EMG data.

As evident from the results, the current model of convolutive mixtures clearly extracted the sources containing tremor compared to the contemporary spectral analysis techniques.

5.0 DISCUSSION AND CONCLUSIONS

5.1 Discussion

In this study, I used the parallel pathway system identification technique to non-invasively characterize the contributions of intrinsic and reflex properties to the stiffness of human joints in Parkinson's disease, with the wrist joint under consideration. The system identification method has been shown to be robust and efficient, with its results being both reliable and repeatable [10] [11]. The results have been reliable for joints such as the ankle [8], shoulder [5], and elbow [6] [7] joints. According to our results, it did a good job to separate the overall torque of the wrist joint into the respective components corresponding to the two parallel pathways as shown in Figure 3.

This method of identification poses a major advantage over those methods determining intrinsic and reflex components by comparing responses before and after removing reflex feedback since those techniques unavoidably involve more time and cannot fully guarantee that any of the intrinsic mechanisms do not get altered during the procedure. Methods involving surgical deafferentation [12], and the ones involving nerve blocks [16], using anesthesia or pressure, need to ensure proper reflex blocking without modifying motor excitations. The factor that might hinder identification in these methods is that different motor units may be active before and after deafferentation and, the aftermath, intrinsic mechanics may change.

Studies postulate that successful parametric system identification involves proper characterization pertinent to the structure of the reflex response and hence the reflex pathway [11]. One of these that can majorly affect the prediction is the reflex delay. Our results support parametric identification with the estimated values of reflex delays in close accordance with those expected for the monosynaptic Ia pathway [10]. The estimated delays take care of all delays associated with the reflex pathway including sensory input from muscle receptors, neural

transmission to the spinal cord and subsequent muscle activation [8] [10] as shown by the results. The considered latency of 40ms ensured none or negligible correlation between the input position and torque due to reflex mechanisms. It can be seen from the predicted torques that the lack of correlation for the considered latency period guarantees that response is due to intrinsic mechanisms only [8] and that the prediction of the reflex torque can be considered a linear additive to the intrinsic torque after the latency period of 40ms.

However, the intrinsic stiffness model required to predict the intrinsic torque from position input needed some improvements in order to elicit its efficacy. Just the discretization of the defined system and subsequently obtaining the model parameters did not cater to the desired response as described earlier. It was found that the system was improper and it was required to add poles to the system to make the system proper and avoid instability. This suggests that the system used to predict the intrinsic torque is somewhat better than the parallel pathway model.

Reflex dynamics were not calculated in this study. However, in conjunction with the assumption of no correlation input position and torque; if the intrinsic stiffness dynamics estimated from the first 40 ms data are predicted by an inefficient model, then they will inevitably affect the estimation of the reflexive stiffness dynamics. Reflex dynamics, in general, would be difficult to describe due to the presence of non-linearity in the reflex pathway. But it can be said that the reflex stiffness will be small at low frequencies and will increase with frequency owing to the presence of differentiator, peak at some frequency and then decrease at higher frequencies due to the presence of low-pass system in the pathway.

One of the factors hindering the outcomes of the work was that the system components comprised in the parallel pathway stiffness model were all in continuous time. The discretization methods employed are believed to be approximations of the continuous time systems and might house some errors. The technique involving discretization using Newton's backward formula used in [2] does not map the left half of s-plane onto the entire unit disc. Tustin's approximation used here in spite of mapping the $j\Omega$ in its entirety to one revolution of the unit disc, the transformation is nonlinear with respect to frequency [25]. The other factors were an inherent bias in the recorded torque data and the effect of initial conditions when considering a perturbation and response segment for identification. It was found that the initial estimates were considerably offset from the desired actual parameter values due to the inherent bias in the Torque. Results improved drastically after cancellation of the bias. The results also did not prove

completely satisfactory without the incorporation of the initial conditions. Each perturbation set had some initial conditions associated with the response which had to be accounted for by calculating the response due to the initial states and then adding them to the final response.

The system identification approach used in this work could also be faced with a few limitations. In such a parametric approach, the model structure chosen for identification has to be known *a priori*. If the structure chosen was not consistent with known anatomy and physiology, and despite the fact other equally appropriate structures are possible, the parameters so estimated and the subsequently predicted responses would lose their biological and physiological credibility. Also, these models might not provide a comprehensive description of joint mechanics as there are a variety of nonlinear effects they do not account for [8]. Thus, the model would change with the operating point governed position, level of activation, perturbation amplitude and a variety of other parameters [10]. Even though a second order model sufficed to characterize stiffness dynamics during stationary conditions, I think the model would become more complex to describe non-stationary changes in joints, for instance, during an imposed stretch [31]. Another important shortcoming could be due to the nature of perturbation. As our neural system is an adaptive controller, they vary their response to the applied signal. We use pseudo-random perturbations to exclude the anticipation of the signal, however, it must be recognized that random perturbations can themselves influence the system. With this knowledge, it can be assumed that the muscles will give resistance despite the pseudo-random nature of perturbation. Consequently, it can be that the prediction of intrinsic response based on the first 40ms data contain some reflexive components. This is supported by my results in which it is evident that the reflexive torque is not strictly zero but hovers around zero with a small value.

The model employed using convolutive mixtures did a successful job in extracting tremor containing sources from the surface EMG signals recorded from different muscles of the forearm. As evident from Figure 15, tremor was better appreciated in the sources extracted using the convolutive mixture model as opposed to direct spectral analysis (using FFT and TFA) on experimentally recorded data. This method provided a good facet to assess tremor found in Parkinson's disease patients and could also serve in the assessment of some higher level neural sources responsible for the generation of such tremor in Parkinson's disease as well as in other movement disorders. This can be of great help to clinicians with patients exhibiting initial symptoms of PD including tremor.

5.2 Conclusions

Although there are some foibles in the parameter estimation procedure and the model used, we obtained reasonably satisfactory results employing the parallel pathway stiffness model. With further improvements, like compliance to nonlinear effect limitations, it would be able to characterize joint mechanics more effectively and would be more meaningful physiologically. Perfection of the model would make way for more effective diagnosis techniques and development of medicinal drugs.

The convolutive mixture model proved successful in the quantification of sources of Parkinsonian tremor from the recorded EMG data. It demonstrated good extraction abilities over the contemporary spectral estimation methods which are in vogue for tremor quantification. This method will be more appreciated by clinicians facilitating their diagnoses as opposed to the clinical rating scales which are presently in use.

BIBLIOGRAPHY

[1] Sherwood, A.M.; Dimitrijevic, M.R., "Brain motor control assessment," *Engineering in Medicine and Biology Society, 1989. Images of the Twenty-First Century., Proceedings of the Annual International Conference of the IEEE Engineering in* , vol., no., pp.943-944 vol.3, 9-12 Nov 1989

[2] Sprague, Chris, "System Identification of Wrist Stiffness in Parkinson's Disease Patients", University of Pittsburgh,PA., 2008

[3] Stiffness: Definition from Answers.com, www.answers.com/topic/**stiffness**-3

[4] Ludvig, D.; Kearney, R.E., "Real-Time Estimation of Intrinsic and Reflex Stiffness," *IEEE Transactions on Biomedical Engineering*, vol.54, no.10, pp.1875-1884, Oct. 2007

[5] F. C. T. van der Helm, A. C. Schouten, E. de Vlugt, and G. G. Brouwn, "Identification of intrinsic and reflexive components of human arm dynamics during postural control," *J Neuroscience Methods*, vol. 119, pp. 1-14, 2002

[6] F. Popescu, J. M. Hidler, and W. Z. Rymer, "Elbow impedance during goal-directed movements," *Exp Brain Res*, vol. 152, pp. 17-28, 2003

[7] D. A. Kistemaker, A. J. V. Soest, and M. F. Bobbert, "Equilibrium point control cannot be refuted by experimental reconstruction of equilibrium point trajectories," *J Neuro-physiol*, vol. 98, pp. 1075-1082, 2007

[8] R. E. Kearney, R. B. Stein, and L. Parameswaian, "Identification of intrinsic and reflex contributions to human ankle stiffness dynamics," *IEEE Trans. Biomed. Eng.*, vol. 44, pp. 493-504, June 1997

[9] Galiana, L.; Kearney, R.E.; Choi, J.; Tung, J.; Fung, J., "Identification of reflex and intrinsic stiffness in spastic stroke ankles," *EMBS/BMES Conference, 2002. Proceedings of the Second Joint* , vol.3, no., pp. 2445-2446 vol.3, 23-26 Oct. 2002

[10] Mirbagheri MM, Barbeau H, Kearney RE, “Intrinsic and reflex contributions to human ankle stiffness: variation with activation level and position”. Exp Brain Res 135:423–436, 2000

[11] Perreault, E.J.; Crago, P.E.; Kirsch, R.F., "Estimation of intrinsic and reflex contributions to muscle dynamics: a modeling study," *IEEE Transactions on Biomedical Engineering*, vol.47, no.11, pp.1413-1421, Nov. 2000

[12] G. C. Agarwal and G. L. Gottlieb, “Effect of vibration on the ankle stretch reflex in man,” *Electroenceph., Clin. Neurophysiol.*, vol. 49, pp.81–92, 1980

[13] J. H. J. Allum, K.-H. Mauritz, and H.Vogele, “The mechanical effectiveness of short latency reflexes in human triceps surae muscles revealed by ischaemia and vibration,” *Exp. Brain Res.*, vol. 48, pp. 153–156, 1982

[14] T. Sinkjaer, E. Toft, S. Andreassen, and B. C. Hornemann, “Muscle stiffness in human ankle dorsiflexors: Intrinsic and reflex components,” *J. Neurophys.*, vol. 60, pp. 1110–1121, 1988

[15] T. Sinkjaer and R. Hayashi, “Regulation of wrist stiffness by the stretch reflex,” *J. Biomech.*, vol. 22, pp. 1133–1140, 1989

[16] Herman R, Freedman W, Mayer N, “Neurophysiologic mechanisms of hemiplegic and paraplegic spasticity: implications for therapy”. Arch Phys Med Rehabil 55:338–343, 1974

[17] Meinders M, Price R, Lehmann JF, Questad KA, “The stretch reflex response in the normal and spastic ankle: effect of ankle position”. Arch Phys Med Rehabil 77:487–492, 1996

[18] Li-Qun Zhang; Rymer, W.Z., "Simultaneous and nonlinear identification of mechanical and reflex properties of human elbow joint muscles", *IEEE Transactions on Biomedical Engineering*, vol.44, no.12, pp.1192-1209, Dec. 1997

[19] Van Den Eden SK, Tanner CM, Bernstein AL, Fross RD, Leimpeter A, Bloch DA, Nelson LM, “Incidence of Parkinson’s Disease: Variation by Age, Gender and Race/Ethnicity”. Am J Epidemiol 157: 1015-1022, 2003

[20] Elble RJ, Pullman SL, Matsumoto JY, Raethjen J, Deuschl G, Tintner R. “Tremor amplitude is logarithmically related to 4- and 5-point tremor rating scales”. Brain 2006; 129: 2660-2666, 2006

[21] Vinjamuri, R.; Crammond, D.J.; Kondziolka, D.; Heung-No Lee; Zhi-Hong Mao, "Extraction of Sources of Tremor in Hand Movements of Patients With Movement Disorders," *Information Technology in Biomedicine, IEEE Transactions on* , vol.13, no.1, pp.49-56, Jan. 2009

[22] S. K. Patrick, A. A. Denington, M. J. A. Gauthier, D. M. Gillard, and A. Prochazka, "Quantification of the UPDRS rigidity scale," *IEEE Transactions on Neural Systems and Rehabilitation Engineering*, vol. 9, no. 1, pp. 31–41, 2001

[23] C. N. Riviere, S. G. Reich, and N. V. Thakor, "Adaptive Fourier modeling of quantification of tremor," *Journal of Neuroscience Methods*, vol. 74, pp. 77–87, 1997

[24] P. E. O'Suilleabhain and J. Y. Matsumoto, "Time-frequency analysis of tremors," *Brain*, vol. 121, pp. 2127–2134, 1998

[25] Alan V Oppenheim, Ronald W Schafer, *Discrete-Time Signal Processing*, 2nd ed., Upper Saddle River, NJ: Prentice Hall, 1999

[26] Haykin, S., "A unified treatment of recursive digital filtering," *Automatic Control, IEEE Transactions on* , vol.17, no.1, pp. 113-116, Feb 1972

[27] Lennart Ljung, *System identification: Theory for the user*, 2nd ed., Publisher: Upper Saddle River, N.J.: Prentice Hall, c1999.

[28] Henry Stark, John W. Woods, *Probability and random processes with applications to signal processing*, 3rd ed., Upper Saddle River, N.J.: Prentice Hall, 2002

[29] M. Castella, S. Rhioui, E. Moreau, and J.-C. Pesquet, "Quadratic higher order criteria for iterative blind separation of a MIMO convolutive mixture of sources," *IEEE Trans. Signal Process.*, vol. 55, no. 1, pp. 218–232, Jan. 2007 (MATLAB Toolbox: http://www-public.int-evry.fr/~castella/toolbox/deflation/deflation.php)

[30] A. Hyvarinen, J. Karhunen, and E. Oja, *Independent Component Analysis*.,New York: Wiley, 2001

[31] Robert F. Kirsch, Robert E. Kearney, "Identification of time-varying stiffness dynamics of the human ankle joint during an imposed movement", *Experimental Brain Research,*vol.114,no.1,pp.71-85, March.1997